JOURNAL OF MATERIALS SCIENCE **36** (2001) 653–662

Electrical, magnetic and Mössbauer properties of cadmium - cobalt ferrites prepared by the tartarate precursor method

A. K. NIKUMBH*, A. V. NAGAWADE, V. B. TADKE, P. P. BAKARE‡
Department of Chemistry, University of Pune, Ganeshkhind, Pune 411 007, India
E-mail: aknik@chem.unipune.ernet.in

Six samples of the system $Cd_{1-x}Co_xFe_2O_4$ were prepared by the tartarate precursor method with $x = 0.0$, 0.2, 0.4, 0.6, 0.8 and 1.0. The formation of ferrispinels were studied by X - ray powder diffraction, infrared spectroscopy, electrical conductivity, thermoelectric power, magnetic hysteresis, initial magnetic susceptibility and Mössbauer spectroscopy. The data of the temperature variation of the direct current electrical conductivity showed a definite kink ($\sim$390°C) except $x = 0.0$ and 0.2, which corresponds to the ferrimagnetic to paramagnetic transitions. Magnetic properties of the samples with $x \geq 0.6$ showed definite hysteresis loops. The observed low magnetic moment can be explained in terms of the non collinear spin arrangement. A well defined hyperfine Zeeman spectra are observed for samples with $x \geq 0.6$ at room temperature and resolved into two sextets corresponding to octahedral and tetrahedral sites. The electrical, magnetic and Mössbauer properties suggest that, a canted spin arrangement upto $x = 0.8$ and Néel's configuration above this composition. The probable ionic configuration for the system is suggested as

$$\left(Cd^{2+}_{1-x}Fe^{3+}_{x}\right)_A \left[Fe^{3+}_{2-x}Co^{2+}_{x}\right]_B O^{2-}_4.$$

1. Introduction

Ferrites are a broad class of complex magnetic oxides of considerable technological importance. The binary and ternary oxides having a spinel structure have attracted wide attention because of their remarkable electrical and magnetic properties [1–4]. These properties are dependent on the nature of the ions, their charges and their distribution among tetrahedral (A) and octahedral (B) sites. This so called cation distribution depends on many factors such as temperature, composition [5–6] and also on the method of preparation of the compounds [7].

Among the various methods of preparation, the coprecipitation (i.e. precursor) technique [8] has attracted laboratory interest because using this method a homogeneity of magnetic particles can be achieved without rigourous and repeated grinding and calcination - normally required in conventional ceramic techniques used in industries. However, systematic studies of the precursor method have also found its identity in industry [9].

In the present work we have prepared the compounds of the system $Cd_{1-x}Co_xFe_2O_4$ by a tartarate coprecipitation technique. We attempted to determine the effect of cadmium ferrite spinel formation and the role of cobalt content on structural and electrical conductivity of these ferrispinels. The magnetic and Mössbauer measurements were also undertaken to study the variation of saturation magnetisation and hyperfine fields with cobalt concentration and to gain information about the cation distributions, possible canted spin structures and supertransferred hyperfine interactions at both A and B sites in the system.

2. Experimental

2.1. Synthesis of precursors

Cadmium - iron - tartarates were prepared by the coprecipitation method by taking high purity (reagent grade) $FeSO_4 \cdot 7H_2O$ (1.86×10^{-1} M/L) and $3CdSO_4 \cdot 8H_2O$ (9.32×10^{-2} M/L) in deionized water. The mixture of metal - sulphate solution was prepared in ratio of $Cd^{2+} : Fe^{2+} = 1 : 2$ with respect to molar ratios and was placed in a three - necked flask under a stream of dry nitrogen. The pH of the medium was adjusted to a low enough value ($pH < 6$), so that hydroxide precipitate does not form. The solution was stirred vigorously with a magnetic stirrer. The sodium tartarate (7.0%) solution was then added slowly with stirring till a permanent precipitate occured. Acetone was added in equal amounts

* Author to whom all correspondence should be addressed.
‡ *Present Address:* SIL, National Chemical Laboratory, Pune 411 008, India.

to metal salts. Here addition of acetone not only ensures a high yield but also influences more homogenous, stoichiometric, fine - grained powders. The resultant precipitate of $CdFe_2(C_4H_4O_6)_3{\cdot}5H_2O$ was light greenish yellow in colour. The solution was filtered after stirring it for 30 minutes. The filtrate was checked for Cd^{2+} and Fe^{2+} whose absence ensured complete coprecipitation. The precipitate was washed several times with cold distilled water and then with acetone to speed - up drying. The precipitate was dried at ambient temperature.

The similar experimental conditions were used for the preparation of cobalt - iron - tartarate, $CoFe_2(C_4H_4O_6)_3{\cdot}7H_2O$ and mixed cobalt - cadmium - iron tartarate, $Co_xCd_{1-x}Fe_2(C_4H_4O_6)_3 \cdot nH_2O$.

2.2. Synthesis of cobalt - cadmium ferrites ($Cd_{1-x}Co_xFe_2O_4$)

For the synthesis of $Cd_{1-x}Co_xFe_2O_4$ ($x = 0.0$ to 1.0), the above tartarate coprecipitates were decomposed and calcined slowly at 700°C for two hours in a platinum crucible under static air atmosphere and then slowly cooled (3°C/min) down to room temperature. This heat treatment is sufficient for achieving a complete decomposition of tartarate. The powder obtained was polycrystallite. This sample was then reground and recalcined at the same temperature for another two hours. The furnace was turned off and sample was removed at room temperature. These samples were stored in a desiccator.

The chemical analysis was done using a Perkin - Elmer Model 3100 Atomic Absorption Spectrometer (AAS) employing an air acetylene flame and a hollow cathode lamp as the light source. The duplicate samples (known amount of $Cd_{1-x}Co_xFe_2O_4$ samples dissolved in 2 ml concentrated HCl and 5 ml HNO_3. The final volume was made to 100 ml) were used for this analysis. A separate lamp was used for the determination of each element. A blank solution (distilled water) was run before and after the aspiration of every sample into flame. The procedures used for the measurements of X - ray diffraction pattern, infrared spectra, d. c. electrical conductivity, magnetic and Mössbauer properties were similar to those reported earlier [10–13]. The Mössbauer spectra were taken at room temperature. The hyperfine interaction parameters were computed using an interactive least square "MOSFIT" Program.

3. Results and discussion

3.1. Characterization of precursors

The elemental analyses made in wt.% of tartarate precursors are very well matched with the calculated ones (Table I). The infrared spectra showed frequencies corresponding to the carboxylate group, hydroxyl group, metal - oxygen etc. The bidentate linkage of tartarate group with metal was confirmed on the basis of the difference between the antisymmetric and symmetric stretching frequencies. There was no bonding with secondary -OH group (of d - tartarate acid) to metal in solid state [14–16]. The X - ray powder diffraction pattern of these precursors showed broad as well as sharp line indicating that the samples were polycrystallite in nature. The presence of water of crystallization was confirmed on the basis of thermal analyses curves.

Thermal decomposition studies of the precursors shows that all the complexes dehydrate and decompose in the temperature range 70 to 400°C. A typical thermogram (TGA and DTG) is shown in Fig. 1. It can be observed that the weight loss in TGA corresponds to the formation of corresponding Cd - Co ferrite, $Cd_{1-x}Co_xFe_2O_4$.

3.2. Characterization of $Cd_{1-x}Co_xFe_2O_4$

3.2.1. X - ray diffraction studies

The compositions of $Cd_{1-x}Co_xFe_2O_4$ samples were determined by atomic absorption spectrometry (AAS). The observed compositions are summarized in Table II. They are found to be ±0.5% of the nominated values. The results of chemical analyses shows that $(Cd_{1-x}Co_x)$: Fe ratio is 1 : 2 within the experimental errors (<1.0%).

The X - ray diffraction patterns of all the compositions indicates the formation of a single spinel phase with cubic structure. No amorphous phase was detected. The experimentally observed d - spacing values

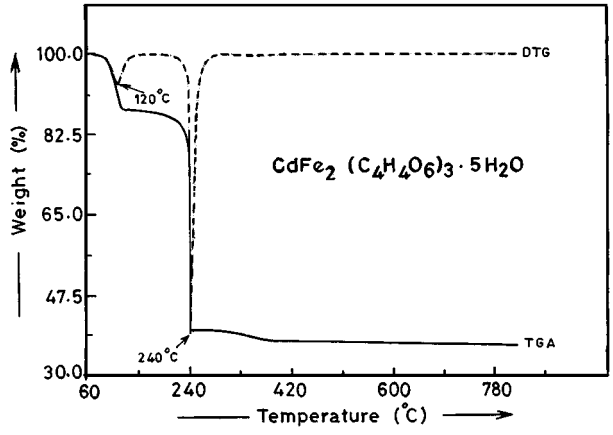

Figure 1 TGA and DTG curves for $CdFe_2(C_4H_4O_6)_3{\cdot}5H_2O$, in static air.

TABLE I Analytical data of tartarate precursors

Precursors	Formula	Formula weight	Elemental analysis in wt. % (±0.5)									
			C		H		Cd		Co		Fe	
			Req.	Found	Req.	Found	Req.	Found	Req.	Found	Req.	Found
Cadmium-iron tartarate pentahydrate	$CdFe_2(C_4H_4O_6)_3{\cdot}5H_2O$	758.1	18.99	18.48	2.90	3.01	14.82	15.41	-	-	14.73	14.24
Cobalt-iron tartarate heptahydrate	$CoFe_2(C_4H_4O_6)_3{\cdot}7H_2O$	740.63	19.44	19.20	1.62	1.70	-	-	7.96	7.91	15.08	14.90

TABLE II Observed chemical analysis of $Cd_{1-x}Co_xFe_2O_4$ ($x = 0.0$ to 1.0)

	Wt. % of (±0.5)					
	Fe		Cd		Co	
Compounds	Found	Req.	Found	Req.	Found	Req.
$CdFe_2O_4$	39.00	38.77	39.31	39.01	-	-
$Cd_{0.8}Co_{0.2}Fe_2O_4$	40.21	40.53	31.41	31.21	4.96	5.02
$Cd_{0.6}Co_{0.4}Fe_2O_4$	42.40	42.30	23.22	23.40	10.06	10.04
$Cd_{0.4}Co_{0.6}Fe_2O_4$	44.31	44.07	15.88	15.60	14.80	15.07
$Cd_{0.2}Co_{0.8}Fe_2O_4$	45.99	45.83	7.65	7.80	19.87	20.09
$CoFe_2O_4$	47.85	47.60	-	-	24.90	25.11

TABLE III X - ray powder diffraction and infrared spectral data for the system $Cd_{1-x}Co_xFe_2O_4$

	X - ray powder diffraction data		Infrared spectral absorption bands (cm^{-1})	
Compounds	Lattice parameter (a) nm.	Mean crystallite size $\langle D\rangle_{X\text{-ray}}$ nm. ± 10%	ν_1	ν_2
$CdFe_2O_4$	0.869	24.29	546	441
$Cd_{0.8}Co_{0.2}Fe_2O_4$	0.860	26.43	553	442
$Cd_{0.6}Co_{0.4}Fe_2O_4$	0.853	28.97	559	448
$Cd_{0.4}Co_{0.6}Fe_2O_4$	0.843	32.35	565	422
$Cd_{0.2}Co_{0.8}Fe_2O_4$	0.837	34.12	574	393
$CoFe_2O_4$	0.835	35.03	574	389

and relative intensities were compared with those reported in literature [17]. The lattice parameter for each composition was then calculated and shown in Table III. The lattice constant values are in the expected range with the lattice constants of $CdFe_2O_4$ [17, 18] and $CoFe_2O_4$ [17, 19] at either end. The crystallite sizes of these samples were calculated from the full width at half - maximums of (220), (311) and (511) diffraction peaks using Debye - Scherrer formula [20]. The mean values of the crystallite diameters $\langle D\rangle_{X\text{-ray}}$ are given in Table III. As can be seen from Table, the mean crystallite size are in the range of 24.29 to 35.03 nm.

The variation of lattice parameter a as a function of cobalt addition x in $Cd_{1-x}Co_xFe_2O_4$ is represented in Fig. 2a. It shows that the lattice parameter decreases linearly with the increase of cobalt content. To confirm this, Wolska *et al.* [21, 22] relation of intensity ratios of X - ray lines was used. In this case, they analysed the intensity ratios of (220) and (422) X - ray lines, dependently only on A - sites, to the weak (222) line, depending only on the cations in octahedral sites, because these ratios are very sensitive to the substitution of Cd^{2+} ions in the B - sites [21, 22]. On the basis of this, in Fig. 3 the recorded sections of observed X - ray powder patterns of $Cd_{1-x}Co_xFe_2O_4$ samples within the 2θ - range of 25–55° are presented. The observed values of these intensity ratios are presented in Fig. 2b. It is observed that these ratios are linearly decreased as x increases i.e. Co^{2+} increases in $Cd_{1-x}Co_xFe_2O_4$ compounds. The electronic configuration of Cd^{2+} ions have a special preference for tetrahedral coordination. This observation is similar to the lattice parameter a as a function of x in $Cd_{1-x}Co_xFe_2O_4$ samples Fig. 2a. Our

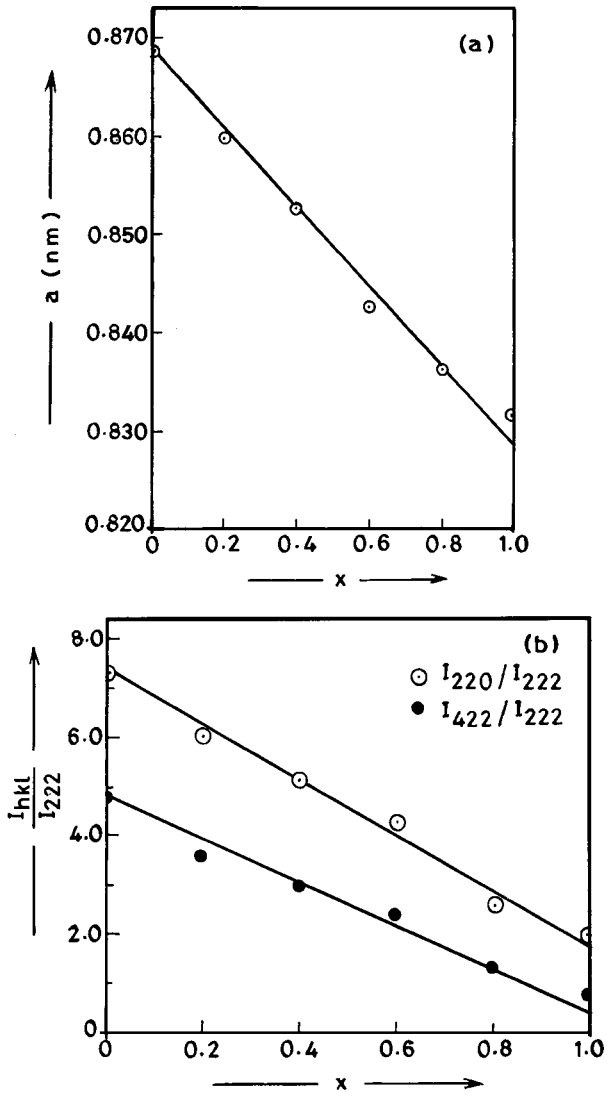

Figure 2 (a) Variation of lattices parameter a as a function of composition x. (b) The ratio of observed intensities of X - ray line I_{220}/I_{222} and I_{422}/I_{222} for the cation distribution of $Cd_{1-x}Fe_x[Co_xFe_{2-x}]O_4$.

results are explained on the assumption that substituting cobalt ions instead of cadmium ions in the composition caused the movement of Fe^{3+} ions from the octahedral site to tetrahedral site. The decrease in lattice constant is also due to the replacement of the smaller Fe^{3+} ion in the octahedral site by comparitively larger Co^{2+} ions [23] i.e. Fe^{3+} has an ionic radius of 0.63 Å and Co^{2+} has an ionic radius of 0.72 Å. In other words replacement of larger Cd^{2+} (ionic radius = 1.03 Å) by comparitively smaller Fe^{3+} in tetrahedral site.

3.2.2. Infrared spectral studies

Infrared spectra of $Cd_{1-x}Co_xFe_2O_4$ samples show two strong bands ν_1 and ν_2 at about 600 and 400 cm^{-1}. The band positions for these compounds are in good agreement with those reported earlier [24, 25]. The band positions are listed in Table III. The band observed at 546 cm^{-1} for $CdFe_2O_4$ (normal spinel) shows a small blue shift on addition of cobalt in the system and changes to $CoFe_2O_4$ (inverse spinel). The absence of the low frequency bands in our compounds suggest that the lattice vibrations which are responsible for these bands are very weak.

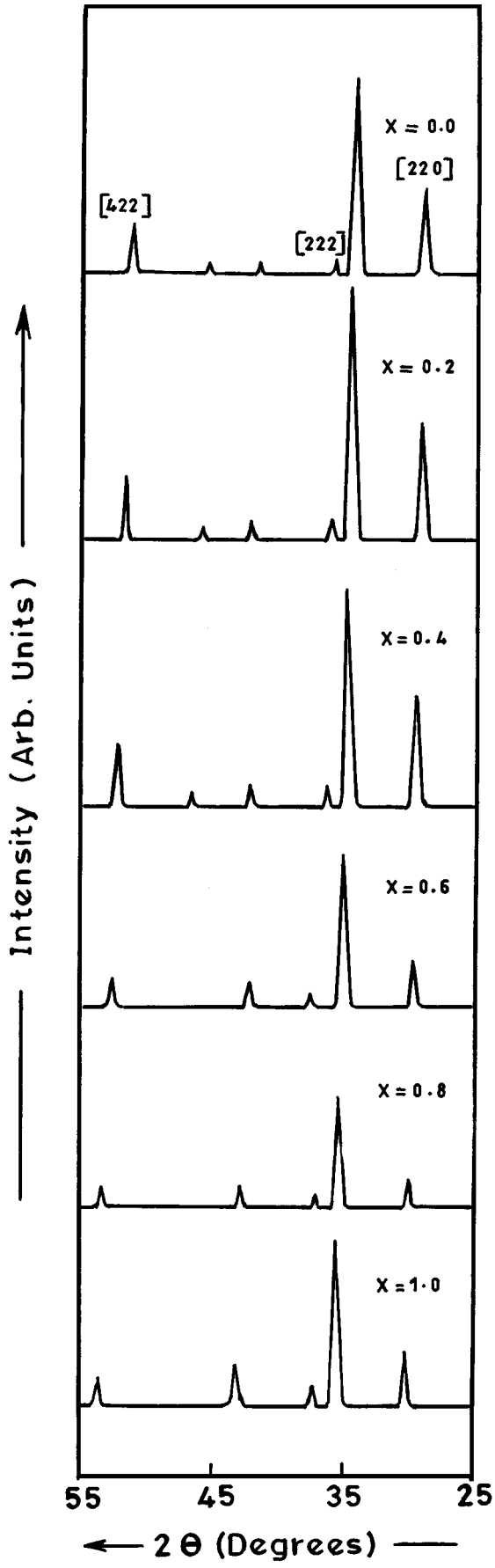

Figure 3 The recorded sections of observed X - ray powder diffraction patterns of $Cd_{1-x}Co_xFe_2O_4$ system.

The presence of Fe^{2+} in the ferrites can cause a shoulder or splitting of the absorption band. Local lattice deformations can occur due to the Jahn-Teller effect in Fe^{2+} which can lead to a non-cubic component in the crystal field potential and to the splitting of the band [26]. The Fe^{2+} ions have an electronic configuration which does not cause Jahn-Teller distortion and hence no splitting is observed.

In the present studies on the infrared spectra of the cadmium - cobalt ferrites reveal that the absorption band around 600 cm^{-1} does not show any splitting or shoulders and the posibility of Fe^{2+} at the A - site is ruled out. There is evidence of a weak shoulder or splitting the absorption band around 400 cm^{-1} suggesting the posible presence of Fe^{2+} at the B-site, but this is not clearly established. The results are in general agreement with literature [25].

Tarte and Coworkers [27] have observed that in ferrites, both the absorption bands depend on the nature of octahedral cations and do not significantly depend on the tetrahedral ions. However, Waldron [28] and Hafner [29] attributed the band ν_1 at around 600 cm^{-1} to the intrinsic vibrations of tetrahedral metal oxygen complexes and the band ν_2 at around 400 cm^{-1} to the intrinsic vibrations of octahedral complexes. The difference in band positions is because of the difference in the $Fe^{3+} - O^{2-}$ distances for the octahedral and tetrahedral complexes.

In an inverse spinel ($CoFe_2O_4$), the octahedral site is occupied by Fe^{3+} and the divalent ion Co^{2+}. Due to charge imbalance the oxygen ion is likely to shift towards the Fe^{3+} ion making the force constant between Fe^{3+} and O^{2-} more. Hence we expect an increase in bond stretching mode, frequencies as we go from normal to inverse spinel. This is supported by our results on $Cd_{1-x}Co_xFe_2O_4$ in which we find that ν_1 increases as x is increased, and ν_2 do not change with the type of spinel structure, given in Table III.

3.2.3. Electrical conductivity and its dependence on composition

The room temperature conducivity values σ_{RT} for all the compounds of the system ($Cd_{1-x}Co_xFe_2O_4$) are found to vary between 10^{-7} and $10^{-8}\Omega^{-1}$ cm^{-1}, for different values of x. High conductivity values indicate that the elements with only one oxidation state are present at the B site. The electrical conductivity - temperature behaviour obeys Wilson's law [30] $\sigma = \sigma_0 \exp(-E_a/KT)$ indicating the semiconducting nature of all the compounds where E_a is the activation energy, K is Boltzmann constant, and T the absolute temperature. The values of log σ were plotted against the reciprocal absolute temperature. The slope of these lines was considered to give the activation energy E_a for the semiconduction of these samples.

The log σ against T^{-1} plot (Fig. 4) of pure $CdFe_2O_4$, $CoFe_2O_4$ and mixed $Cd_{1-x}Co_xFe_2O_4$ shows an initial decrease in electrical conductivity in the temperature range 60–140°C. The σ value then increases showing a definite kink (brake) at about 390°C except $CdFe_2O_4$ and $Cd_{0.8}Co_{0.2}Fe_2O_4$, on further increase of temperature the σ value increases as temperature increases. The decrease in conductivity in the temperature range of 60–140°C (Table IV) corresponds to the desorption of absorbed water molecules, usually absorbed water molecules behave as an electron donor. The kink occurs

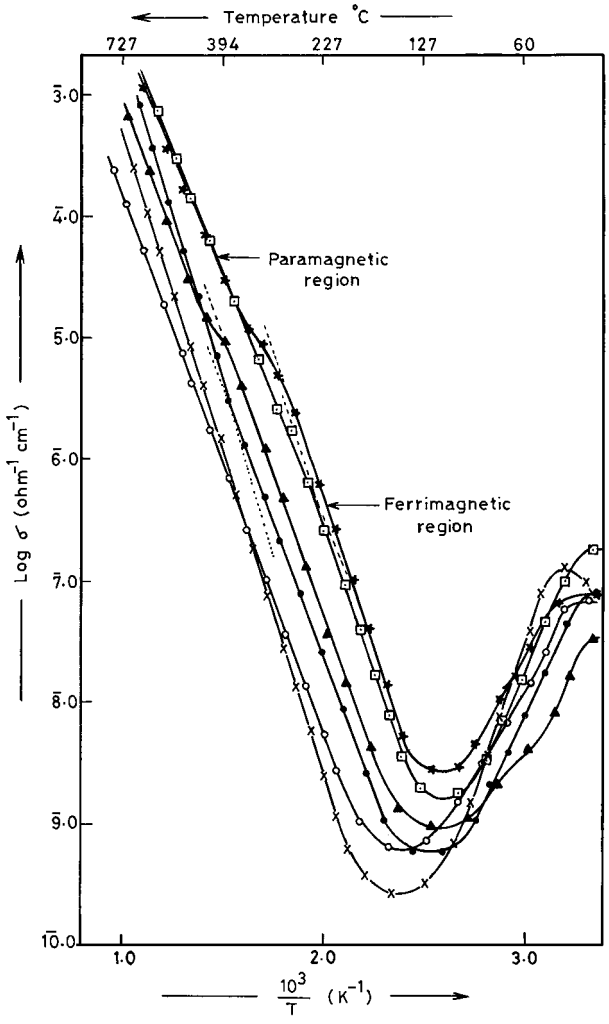

Figure 4 Plot of log σ against T^{-1} of $Cd_{1-x}Co_xFe_2O_4$. ○, $x = 0$; ×, $x = 0.2$; ●, $x = 0.4$; ▲, $x = 0.6$; ⊡, $x = 0.8$ and ∗, $x = 1.0$.

in each curve, at temperature which corresponds to ferrimagnetic (ordered state) to paramagnetic transition (disordered state). No such magnetic transformation was observed for the samples $CdFe_2O_4$ and $Cd_{0.8}Co_{0.2}Fe_2O_4$, suggesting that these samples are paramagnetic at room temperature. The kink will be most marked for those cases (i.e. $x \geq 0.4$) in which there is a strong exchange interaction between the outer and inner electrons. Irkhin and Turov [31] have proposed a theoretical explanation for the existence of kinks at the ferrimagnetic to paramagnetic transition temperature (T_C). They conclude that the activation energy and the effective mass of current - carrying excitons in ferromagnetic semiconductor depend on the spontaneous magnetization because of a "magnetizing" exchange interaction between the outer and inner electrons. This leads to an additional temperature dependence of the electrical resistance which is particularly strong near T_C.

The two activation energies are calculated for the two regions around the kink points, firstly for ferrimagnetic and secondly for paramagnetic region. The calculated values of the activation energies, E_a (eV), for the series $Cd_{1-x}Co_xFe_2O_4$ are listed in Table IV. It is interesting to observe here that the activation energy in the paramagnetic region is higher than that in the ferrimagnetic region. The behaviour of the activation energy on passing through T_C may be explained by the double exchange mechanism [31]. Hence the electrical conduction in the system under investigation is due to the electron hopping in the sublattices between $Fe^{2+} \rightleftarrows Fe^{3+}$ ions and results increasing in activation energy in the paramagnetic region. It can also be seen that the conductivity increasing with the increase of cobalt concentration (Fig. 4). This may be due to the presence of a large number of cobalt ions (which can show the Co^{2+} to Co^{3+} mechanism) in the sample.

The increase in E_a with increasing x (Table IV) can be interpreted in terms of their magnetic properties. However, in case of $Cd_{1-x}Co_xFe_2O_4$ samples the magnetic ordering changes occur at about $x \geq 0.4$, which might be responsible for this increase in the activation energy. This is further confirmed by studying the saturation magnetization in these samples. Néel [32] has explained the magnetic behaviour of these spinels on the basis of exchange interactions that occur between the transition - metal ions at A and B sites in the spinel structure. The three possible interactions are A - A, A - B and B - B. The relative magnitude of interaction was found to be in the order : AB > BB > AA. In $CdFe_2O_4$ spinels all the three exchange interactions are present and are normally antiferromagnetic [33]. The activation energy for this sample is much lower owing to very weak A - B interactions (Cd^{2+} nonmagnetic). As the cobalt concentration (x) increases in the $Cd_{1-x}Co_xFe_2O_4$ mixed spinels, the antiferromagnetic order changes and enhances the activation energy for electrical conduction. Therefore, the magnetic ordering changes might be responsible for the increase in the activation energy. For $CoFe_2O_4$ spinel, Co^{2+} and Fe^{3+} cations are found to be equally distributed in the octahedral lattice site. As hopping between ions of different metals on the octahedral sublattices [34] needs higher

TABLE IV D. C. electrical conductivity data of $Cd_{1-x}Co_xFe_2O_4$

Compounds	Temperature, corresponding to desorption of absorbed H_2O (K)	σ at 500 K Ω^{-1} cm^{-1}	Activation energy Ea (±0.02 eV)	
			Ferrimagnetic region	Paramagnetic region
$CdFe_2O_4$	416	4.63×10^{-8}	-	0.886
$Cd_{0.8}Co_{0.2}Fe_2O_4$	413	2.71×10^{-8}	-	0.899
$Cd_{0.6}Co_{0.4}Fe_2O_4$	300	1.26×10^{-7}	0.875	0.909
$Cd_{0.4}Co_{0.6}Fe_2O_4$	380	5.84×10^{-7}	0.916	0.923
$Cd_{0.2}Co_{0.8}Fe_2O_4$	370	1.84×10^{-6}	0.945	0.954
$CoFe_2O_4$	375	2.51×10^{-6}	0.970	0.982

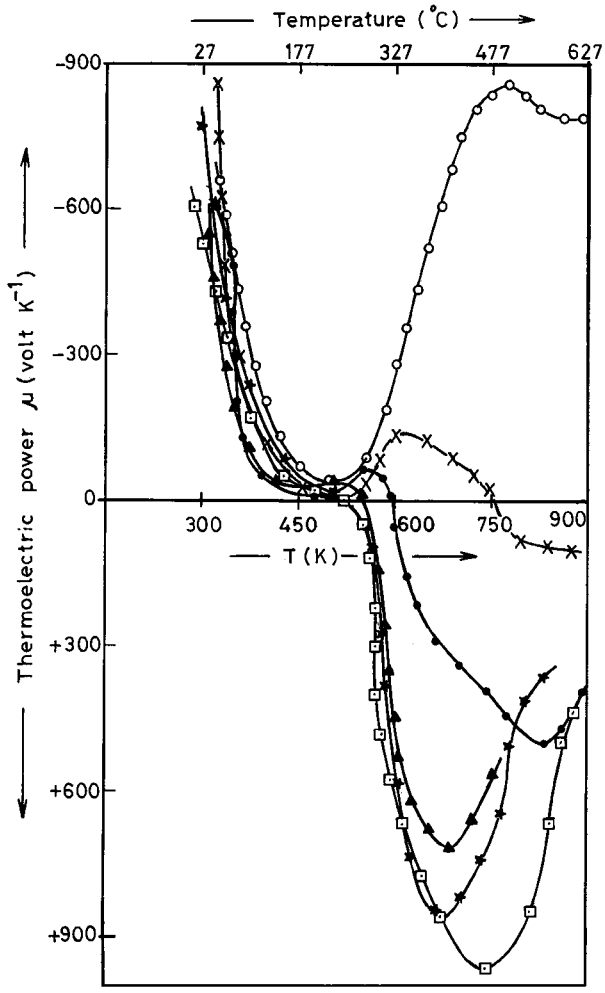

Figure 5 Plot of thermoelectric power, μ (volt K^{-1}) against, T (K) of $Cd_{1-x}Co_xFe_2O_4$. 0, $x = 0$; ×, $x = 0.2$; ●, $x = 0.4$; ▲, $x = 0.6$; ⊡, $x = 0.8$ and ∗, $x = 1.0$.

activation energy than for ions of the same metal. Thus conduction activation energy for $CoFe_2O_4$ is higher.

3.2.4. Thermoelectric power measurements

The thermoelectric power measurements for $Cd_{1-x}Co_xFe_2O_4$ in Fig. 5 shows an initial fall in the number of charge carriers (negative change carriers) in the temperature range up to 425 K and the number then remains almost constant up to 500 K. After this, for $x = 0$, the negative thermoelectric power increases in magnitude with increasing temperature. Similarly for $x = 0.2$ and 0.4, the negative thermoelectric power increases slightly and then decreases to become positive at higher temperature. While, for $x \geq 0.6$, the negative thermoelectric power becomes positive and its magnitude increases with increasing temperature.

The thermoelectric power for $Cd_{1-x}Co_xFe_2O_4$ ($x = 0$ to 1) samples is negative (n - type) indicating that electrons are majority carriers up to 500 K. This might be due to activated electron hopping between Fe^{2+} and Fe^{3+}. Above 500 K thermoelectric power becomes positive except for $x = 0$, indicating that the majority of carriers are holes. It is interesting to observe here that the positive thermoelectric power increases with increasing concentration of cobalt in the system. Thus the jumping of holes between Co^{3+} to Co^{2+} ions is a prominent conduction mechanism in the system containing higher concentration of cobalt. So the low conductivity of the mixed system may be due to electron - hole compensation.

3.2.5. Magnetic studies

The compounds of the system $Cd_{1-x}Co_xFe_2O_4$ with $x \geq 0.6$ studied in the present work showed a definite hysteresis loop at room temperature, which indicates the ferrimagnetic behaviour. From the hyteresis loops, the coercive force (Hc), saturation magnetization (Ms), ratio of remanance to sturation magnetization (M_R/M_S), magnetic moment (n_B) and YK angles (θ_{YK}) values have been listed in Table V. It is interesting to observe that the Hc, Ms and M_R/M_S increase as cobalt content ($x \geq 0.6$) increases for $Cd_{1-x}Co_xFe_2O_4$ samples. The compounds, with $x = 0.0$ and 0.2 do not show hysteresis loop indicating that these ferrites are antiferromagnetic in nature. Since cadmium ferrite ($x = 0$) is known to have the normal spinel - type structure, i.e. the divalent ions (Cd^{2+}) occupy mainly tetrahedral sites. In addition to Cd^{2+}, the tetrahedral interstices also contain smaller Fe^{3+} ions. Therefore B - B interaction is prominent in these samples. The sample with $x = 0.4$ showed negligible saturation magnetization as compared to other mixed $Cd_{1-x}Co_xFe_2O_4$ samples, where $x \geq 0.6$. This low value is due to non - uniformity, so that the sample consisted of a mixture of a paramagnetic phase (as the major phase) and a small amount of a ferrimagnetic phase at room temperature. The saturation magnetization with $x > 0.8$ are in full agreement with the Néel theory of ferrimagnetism [32]. The introduction of cobalt ions, which have a strong preference for the spinel B - sites and the cation distribution is given by

$$\left(Cd^{2+}_{1-x}Fe^{3+}_{x}\right)\left[Fe^{3+}_{2-x}Co^{2+}_{x}\right]O^{2-}_{4}$$

TABLE V Magnetic properties and curie temperature (T_c) for $Cd_{1-x}Co_xFe_2O_4$

Compounds	Coercive force (H_c) ± 25 Oe	Saturation magnetisation (M_s) ± 2 emu g^{-1}	Ratio of M_R/M_S	Magnetic moment $n_B \pm 0.1$ μB		$\langle\theta\, YK\rangle$ observed	Curie temperature (T_c) ± 5 K
				Observed	Calculated		
$CdFe_2O_4$	-	-	-	-	-	-	-
$Cd_{0.8}Co_{0.2}Fe_2O_4$	-	-	-	-	-	-	-
$Cd_{0.6}Co_{0.4}Fe_2O_4$	850	7.01	0.33	0.33	8.65	72° 10′	625
$Cd_{0.4}Co_{0.6}Fe_2O_4$	400	75.0	0.46	3.44	7.06	29° 50′	685
$Cd_{0.2}Co_{0.8}Fe_2O_4$	525	70.0	0.51	3.07	5.46	10° 73′	725
$CoFe_2O_4$	675	92.0	0.64	3.87	3.87	0	765

where the ions enclosed by round brackets correspond to tetrahedral or A-site and the ions enclosed by square brackets corresponds to octahedral or B-site. Magnetization is, therefore, given by

$$3.87x + 5.92(2-x) - 5.92(x) = 3.87x + 11.84(1-x)$$

by considering the magnetic moment of the Co^{2+} ions of the order of 3.87 μ_B and that of the Fe^{3+} ions of 5.92 μ_B. The substitution of paramagnetic Co^{2+} ions at B sites we observed that some Fe^{3+} ions started to migrate to the A - site and hence strengthening the A - B interaction. When 50% of the B - sites are substituted by Co^{2+} ions, the B-B interaction becomes comparable in strength to A - B interaction. B spins are then longer parallel and the net magnetic moment increases.

The magnetic moment n_B per formula unit has been calculated from the saturation magnetization (M_S) value at room temperature by using the relation

$$n_B = \frac{\text{Molecular weight} \times \text{Saturation magnetization}}{5585}$$

The observed n_B values obtained by this equation are compared with the calculated n_B values on the basis of spin - only moments of Néel's [32] two sub - lattice model (Table V). It has been observed that in case of $x = 1$ (i.e. $CoFe_2O_4$) the observed and calculated magnetic moments are very similar to each other. The observed n_B values for $x \geq 0.4$ are lower than the calculated n_B values (Table V). These low magnetic moments can be explained in terms of the non - collinear spin arrangement i.e. the presence of a small canting of the B site moment with respect to the direction of the A site moment [2, 35]. The Yafet - Kittel angles (θ_{YK}) were calculated by using the relation given in the literature [35, 36] and are listed in Table V. Thus the observed variation of the saturation magnetization with cadmium concentration has been explained on the basis of the existence of Yafet - Kittel angles on the B site spins. The observed variation may be due to the preparation techniques.

All compounds possess high values of coercive force (Hc), which may be due to the presence of anisotropy in these compounds. A large increase in Hc is indicative of single - domain behaviour [37]. The presence of single - domain particles in $Cd_{1-x}Co_xFe_2O_4$ compounds with $x \geq 0.4$ is also confirmed by the considerable increase (Table V) in the remanance ratio M_R/M_S at room temperature. It is interesting to observe that, for all samples the M_R/M_S ratio, increasing with increase of mean crystallite size (see Table III) is rather unusual. One possible explanation could be as follows.

For all samples, the single domain particles are larger and the contribution of the uniaxial anisotropy due to the internal strains diminishes, there anisotropy approaches the cubic type value, which leads to decrease of Hc. In this way, the magnetic behaviour of the system approaches that of a random system of non - interacting single - domain particles with cubic anisotropy, exhibiting values of M_R/M_S ratio greater than 0.5. The room temperature (RT) single - domain diameter, estimated by the Kittel formula, is 100 nm and the RT superparamagnetic diameter, estimated by the Néel theory, is 10 nm [38]. The RT critical single - domain size, reported on the basis of coercivity measurements, is of the order of 70 nm [39–41].

3.2.6. Initial magnetic susceptibility

The study of the temperature variation of initial magnetic susceptibility (χ_i) curves of $Cd_{1-x}Co_xFe_2O_4$ ($x \geq 0.4$), compounds show a typical Hopkinson effect [42]. For these samples, χ_i increases with increasing temperature giving a broad peak value and then suddenly become zero just before the Curie temperature (Fig. 6). This is a characteristic behaviour of samples having a single domain grains. The Curie temperature (Tc) for $x \geq 0.4$ compounds are determined from these curves and are listed in Table V. Tc values are found to increase with increasing Co^{2+} concentration at B - site,

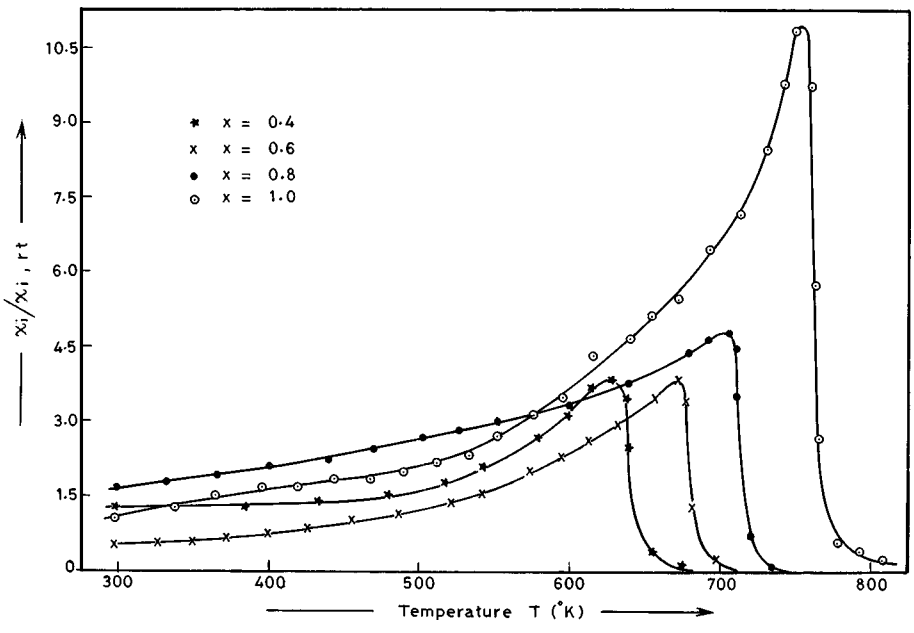

Figure 6 Plot of x_i/x_i, rt against T for the system $Cd_{1-x}Co_xFe_2O_4$.

probably due to the strengthening of the A - B interactions. The absence of multi - domain grains is supported by the fact that Hopkinson's effect is not observed.

For $x = 0.0$ and 0.2, no Curie temperatures are observed at and above room temperature. This suggests that for $x = 0.2$, the Curie temperature may be below room temperature (25°C). To support this, the hysteresis loop experiment was carried out at liquid nitrogen temperature. At the low temperature a saturation magnetiztion ($M_S = 12.4$ emug^{-1}) was observed.

3.2.7. Mössbauer studies

The room temperature Mössbauer spectra of $CdFe_2O_4$, $CoFe_2O_4$ and mixed ferrite $Cd_{1-x}Co_xFe_2O_4$ are shown in Fig. 7 and the spectral parameters such as isomer shift

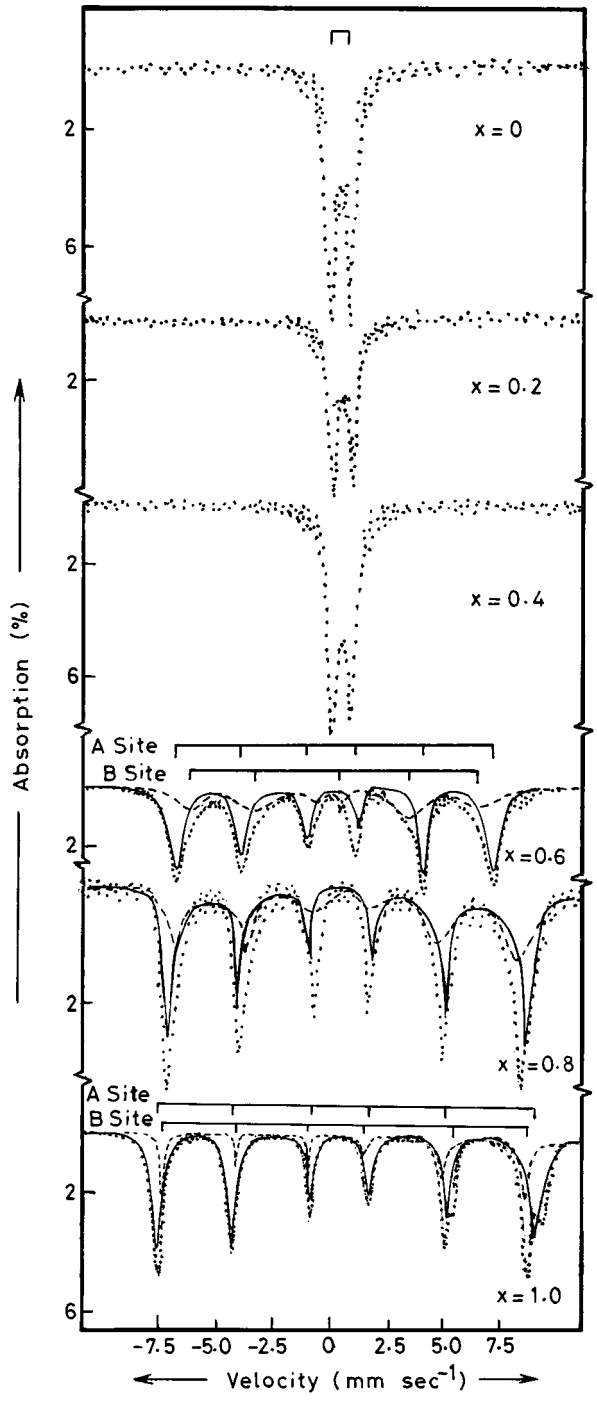

Figure 7 Mössbauer spectra at room temperature of $Cd_{1-x}Co_xFe_2O_4$.

(δ), quadrupole splitting (ΔE_Q) and hyperfine fields (H_n) at A and B sites are computed and are summarised in Table VI. In the Fig. 7, the black dots represent the experimental points and continuous line and the dashlines through the data point are results of the least squares fit to the data of the two mixed magnetic dipole and electirc quadrupole ^{57}Fe hyperfine pattern of each other.

The isomer shift is a useful parameter in identifying the spectra due to A and B site Fe^{3+} ions. Because of the difference in Fe^{3+}—O^{2-} distance for the two sites, isomer - shift is expected to be different. The isomer shift show very little change (Fig. 8a) with Co^{2+} content upto $0.0 \leq x \leq 0.4$, indicating that the S - electron distribution of Fe^{3+} ions is practically not influenced by Co^{2+} substitutions. It is also apparent from Table VI that $x = 0.6$ and 0.8 have significant variation of isomer shifts for Fe^{3+} ions at A and B site. This indicates that the S - electron distribution of the Fe^{3+} ions is very much influenced by Co^{2+} substitution at B - site.

The Mössbauer spectra of $Cd_{1-x}Co_xFe_2O_4$ with $x = 0$ to 0.4 (Fig. 7) are paramagnetic at room temperature. However, for $x = 0.4$ showed negligible saturation magnetization, this is due to the sample consisted of a paramagnetic as the major phase or more probaly, that instead of ferrimagnetic particles in this case ferromagnetic regions exist which are separated magnetically from the matrix, since the region is surrounded by diamagnetic Cd^{2+} ions. In the case of $Cd_{0.8}Co_{0.2}Fe_2O_4$ and $Cd_{0.6}Co_{0.4}Fe_2O_4$, there is a small percentage of Fe^{3+} ions at A - sites which do not experience any electric field gradient due to cubic symmetry of this site. Hence the spectrum has been split into a singlet arising from A - site and a doublet corresponding to B - site iron.

The plot of quadrupole splitting against cobalt content (x) are shown in Fig. 8b. It is seen that the pure $CdFe_2O_4$ shows the highest value of quadrupole splitting, while $x \geq 0.6$ have practically no quadrupole splitting (Table VI), which suggests that coexistence of chemical disorder and over all cubic symmetry causes no net quadrupole splitting. This supports the result of Bayukov *et al.* [43].

The Mössbauer spectra of $Cd_{1-x}Co_xFe_2O_4$ with $x \geq 0.6$ (Fig. 7) exhibit normal Zeeman split sextets, one due to Fe^{3+} ions at the tetrahedral (A) sites and the other due to Fe^{3+} ions at the octahedral (B) sites. The compounds with $x \leq 0.4$ show paramagnetic doublets i.e. no distinct evaluation of the hyperfine field observed. The observed variation of A and B site hyperfine fields (H_n) with the cobalt concentration ($x \geq 0.6$) is shown in Fig. 8c. This is attributed to exclusive octahedral site occupation of Co^{2+} cations. The B site hyperfine field increases because of increasing magnetization of the B sublattice. The magnetic measurements confirmed this result.

It is also apparent that A - site hyperfine field (H_A) increases faster than B-site hyperfine field (H_B) Fig. 8c. This may be possible due to a change in spin orientations in cobalt substituted ferrites. It is interesting to observe that with increasing x (i.e. cobalt content), the lattice parameter decreases and the overlap of electron wave function of Fe^{3+} ions and O^{2-} ions increases and the hyperfine field increases. Since with increase in Co^{2+} content the mean splitting increases (as the Curie

TABLE VI Mössbauer parameter for $Cd_{1-x}Co_xFe_2O_4$

Compounds	Site	Isomer shift*, (δ) ($\pm$0.02 mm sec^{-1})	Quadrupole splitting, (ΔEQ) ($\pm$0.02 mm sec^{-1})	Hyperfine field, (Hn) ($\pm$5.0 KOe)
$CdFe_2O_4$	-	0.35	0.81	-
$Cd_{0.8}Co_{0.2}Fe_2O_4$	-	0.36	0.84	-
$Cd_{0.6}Co_{0.4}Fe_2O_4$	-	0.37	0.87	-
$Cd_{0.4}Co_{0.6}Fe_2O_4$	A	0.40	0.05	417
	B	0.53	0.06	459
$Cd_{0.2}Co_{0.8}Fe_2O_4$	A	0.38	0.06	449
	B	0.61	0.11	486
$CoFe_2O_4$	A	0.36	0.07	505
	B	0.70	0.16	519

*With respect to natural iron metal.

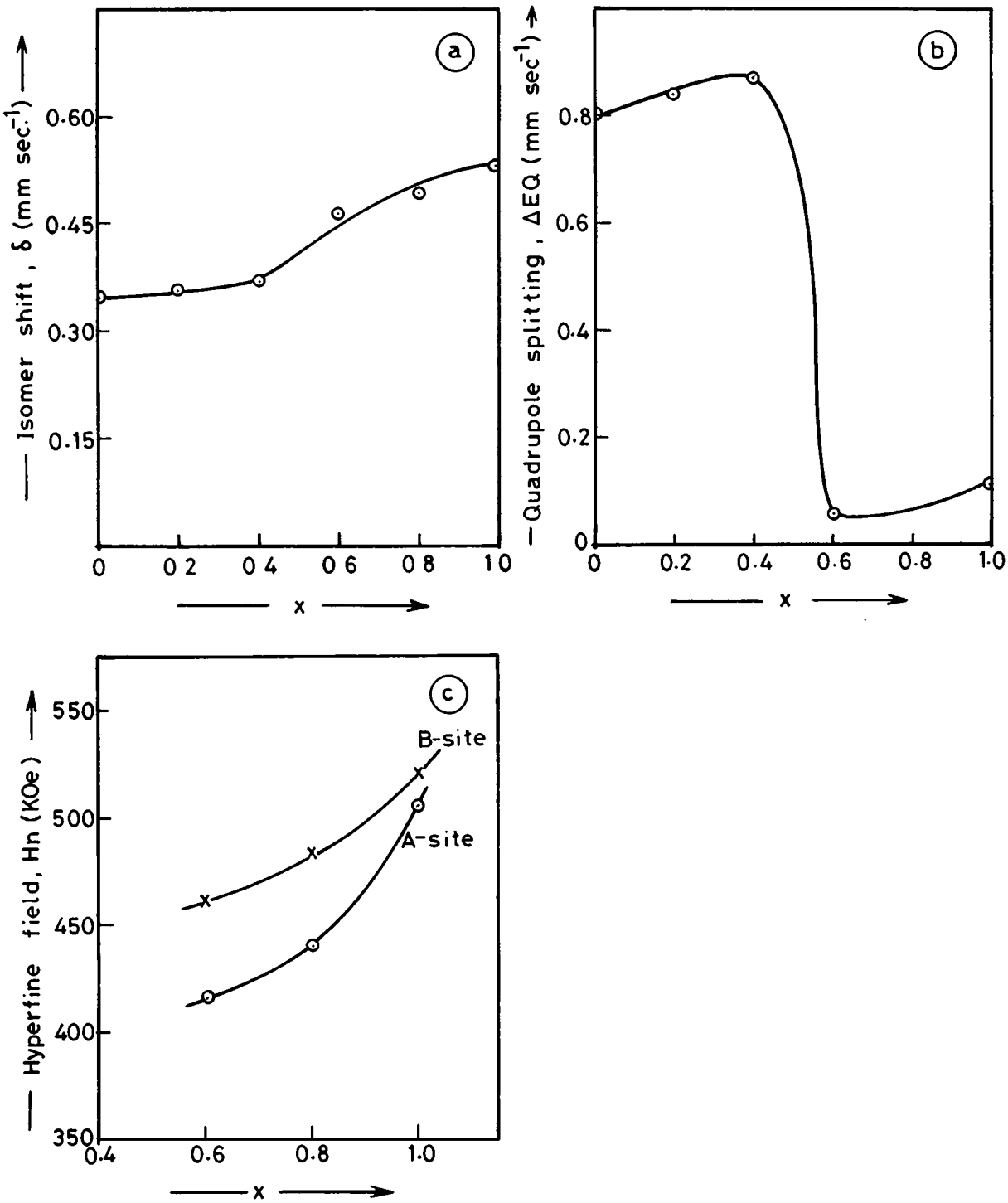

Figure 8 Variation of ⓐ- Isomer shift; ⓑ- quadrupole splitting and ⓒ- hyperfine field with x in $Cd_{1-x}Co_xFe_2O_4$ system.

temperature does, the magnetic coupling strengthens the A - B interactions). Thus the sextets with a higher magnetic splitting (H_B) belong to Fe^{3+} environments in which the number of neighbouring Co^{2+} is larger (i.e. superexchange interactions Fe^{3+}–O–Co^{2+} increases). Hence we think that the canted spin arrangement (i.e. Yafet - Kittel angles) may be present in $Cd_{1-x}Co_xFe_2O_4$ upto $x = 0.8$ which suggests that B - B and A - B superexchange interactions are comparable in strength. The Néel two sublattice model may be applicable upto $x > 0.8$ cobalt content.

4. Conclusions

(a) Temperature variation of direct current electrical conductivity of pure $CoFe_2O_4$ and mixed $Cd_{1-x}Co_xFe_2O_4$ show a definite kink except pure $CdFe_2O_4$, which corresponds to ferrimagnetic to paramagnetic transitions. The activation energy in the paramagnetic region is higher than the ferrimagnetic region.

(b) The thermoelectric power for $Cd_{1-x}Co_xFe_2O_4$ ($x = 0.0$ to 1) samples are of negative sign at room temperature. It increases in magnitude with temperature in the ferrimagnetic region and becomes positive above 500 K except for $x = 0$.

(c) The compounds of the system $Cd_{1-x}Co_xFe_2O_4$ with $x \geq 0.6$ showed a definite hysteresis loop. The coercive force, saturation magnetization and the ratio of remanance to saturation magnetization (M_R/M_S) increases as cobalt content increases.

(d) The data on the temperature variation of the initial magnetic susceptibility suggest that these samples have single domain grains. The Curie temperature are found to increase with increasing Co^{2+} content.

(e) The Mössbauer spectra of $Cd_{1-x}Co_xFe_2O_4$ with $x = 0.0$ to 0.4 shows a paramagnetic doublets while with $x \geq 0.6$ exhibits normal Zeeman split sextets at room temperature. The systematic increase in hyperfine field at both sites and the rapid increase at tetrahedral (A) site as compared to that at octahedral (B) site in $x \geq 0.6$ samples have been suggested that the magnetic coupling strengthens A - B interactions. The canted spin arrangement may be present in these compounds.

(f) By means of the electrical, magnetic and Mössbauer results, the cation distribution has been found to be

$$\left(Cd^{2+}_{1-x}Fe^{3+}_{x}\right)_A \left[Fe^{3+}_{2-x}Co^{2+}_{x}\right]_B O^{2-}_4.$$

Acknowledgements

This work was supported by U.G.C., New Delhi. The teacher fellowship scheme (AVN) was awarded. The authors wish to thank Dr. S. K. Date. Physical Chemistry Division, National Chemical Laboratory, Pune, for facilities given for part of the work.

References

1. J. SMIT and H. P. J. WIJN, "Ferrites" Physical Properties of Ferrimagnetic Oxides in Relation to Their Technical Applications. Endhover : Philips (1959).
2. J. B.GOODENOUG, *Prog. Solid State Chem*. **5** (1971) 146.
3. C. P. POLLE and H. A. FARACH, *Z. Phys. B*. **47** (1982) 55.
4. D. J. CRAIK, "Magnetic Oxides, Vol. 2" (Wiley - Interscience, New York, 1975).
5. M. SCHMALZARIED, *Z. Phys. Chem*. **28** (1961) 203.
6. R. K. DALTA and R. ROY, *J. Amer. Ceram. Soc*. **50** (1967) 578.
7. N. YAMAMOTO, S. KAWANA, N. ACHIWA, M. KIYAMA and T. TAKADA, *J. Appl. Phys*. **12** (1973) 1830.
8. W. J. SCHULLE, *J. Phys. Chem*. **68** (1959) 83.
9. J. TETSUO, S. MASAHIRO, I. NOBUO and S. TOSHIHIKO, *Chem. Abstr*. **110** (1988) 127355q.
10. A. K. NIKUMBH, K. S. RANE and A. J. MUKHEDKAR, *J. Mater. Sci*. **17** (1982) 2503.
11. K. S. RANE, A. K. NIKUMBH and A. J. MUKHEDKAR, *ibid*. **16** (1981) 2387.
12. A. K. NIKUMBH, *ibid*. **25** (1990) 3773.
13. A. K. NIKUMBH, M. M. PHADKE and A. A. LATKAR, *J. Magn. Magn. Mater*. **131** (1994) 189.
14. K. NAKAMOTO, "Infrared Spectra of Inorganic and Coordination Compounds," 2nd ed. (Wiley - Interscience, New York, 1970) p. 244.
15. V. FREI and J. EDEROVA, *J. Collect. Czech. Chem. Comm*. **34** (1969) 1304.
16. S. KRISHNER and R. KIASLING, *J. Amer. Chem. Soc*. **82** (1960) 4174.
17. ASTM File number 22 - 1063.
18. A. A. GHANI and A. A. SATTAR, *J. Magn. and Magn. Mat*. **97** (1991) 141.
19. P. NATHWANI and V. S. DARSHANE, *J. Phys. C*. **21** (1988) 3191.
20. H. P. KLUG and L. E. ALEXANDER, "X - ray Diffraction Procedure" (Wiley - Interscience, New York, 1954) Ch. 9.
21. E. WOLSKA, E. RIEDEL and W. WOLSKI, *Phys. Status. Solidi (A)* **132** (1992) K 51.
22. *Idem., Solid State Ionics* **51** (1992) 231.
23. R. D. SHANNON and C. T. PREWITT, *Acta. Crystallogr. B* **26** (1970) 1076.
24. T. T. SRINIVASAN, C. M. SRIVASTAVA, N. VENKATRAMANI and M. J. PATNI, *Bull. Mat. Sci*. **6** (1984) 1063.
25. M. M. GIRGIS and A. M. EL. AWAD, *Mat. Chem. and Phys*. **36** (1993) 48.
26. V. R. BOTAKOVA, N. D. ZERVEY and V. P. ROMANOV, *Phys. Status Solidi (A)* **12** (1972) 623.
27. P. TARTE and R. COLLONGUES, *Ann. Chim. Paris*. **9** (1964) 135.
28. R. D. WALDRON, *Phys. Rev*. **99** (1955) 1727.
29. S. HAFNER, *Z. Kristallorg*. **115** (1961) 331.
30. S. R. MORRISON, *The Chem. Phys. of Surface, Plenum* (1977) 70.
31. YU. P. IRKHIN and E. A. TUROV, *Sou. Phys-JETP* **33** (1957) 673.
32. L. NEEL, *Ann. Phys*. **3** (1948) 137.
33. P. I. SLICK in E. P. WOHLFARTH (eds.) "Ferromagnetic Materials, Vol. 2" (North Holland, Amsterdam, 1980) Ch. 3.
34. C. C. WU, S. KUMARKRISHANAN and T. O. MASON, *J. Solid State Chem*. **37** (1981) 144.
35. Y. YAFET and C. KITTEL, *Phys. Rev*. **87** (1952) 290.
36. V. G. PANICKER, R. V. UPADHYAY, S. N. RAO, R. G. KULKARNI, *J. Mater. sci. Lett*. **3** (1984) 385.
37. C. P. BEAN, *J. Appl. Phys*. **26** (1955) 1381.
38. D. J. DUNLOP, *Phil. Mag. Ser*. **9** (1969) 239.
39. A. E. BERKOWITZ and W. J. SCHUELE, *J. Appl. Phys*. **30** (1959) 1345.
40. E. P. WOHLFARTH, *J. Phys. Radium* **20** (1959) 295.
41. M. GRIGOROVA, H. J. BLYTHE, V. BLOSKOV, V. RUSANOV, V. PETKOV, V. MASHEVA, D. NIHITIANOVA, LL. M. MARTINEZ, J. S. MUNOZ and M. MIKHOV, *J. Mag. Magn. Mater*. **183** (1998) 163.
42. J. HOPKINSON, *Phil. Trans. R. S. (London) A* **180** (1889) 443.
43. O. A. BAYUKOV, V. P. IKONNIKOV, G. N. ILINOVA and G. P. POPOV, *Sov. Phys. Solid St*. **14** (1973) 2040.

Received 15 September 1999
and accepted 23 March 2000